A NUMERICAL STUDY OF THE BREAK DOWN OF INVARIANT TORI IN 4D SYMPLECTIC MAPS*

A. Haro and C. Simó

Departament de Matemàtica Aplicada i Anàlisi
Universitat de Barcelona
Gran Via, 585, Barcelona, Spain
E-mail: `haro@cerber.mat.ub.es`, `carles@maia.ub.es`

1 Standard-like maps in the polycylinder

1.1 The polycylinder

Let $\mathbf{T}^d = \mathbf{R}^d/\mathbf{Z}^d$ be the *d-torus*, and let $\mathbf{A}^d = \mathbf{T}^d \times \mathbf{R}^d$ be the *d-cylinder* (or d-annulus). The coordinates on $\mathbf{A}^d$ are $(x(\text{mod } 1), y)$ (*angle* - *action* coordinates).

1.2 Standard-like maps

In what follows we shall consider diffeomorphisms on the d-cylinder

$$f : \mathbf{T}^d \times \mathbf{R}^d \to \mathbf{T}^d \times \mathbf{R}^d$$

having a *lift*:

$$F : \mathbf{R}^d \times \mathbf{R}^d \to \mathbf{R}^d \times \mathbf{R}^d$$

of the form:

$$\left\{ \begin{array}{l} x' = x + y + \Omega(x), \\ y' = y + \Omega(x), \end{array} \right.$$

where $\Omega = -\nabla V$ and $V : \mathbf{R}^d \to \mathbf{R}$ is a 1-periodic function in all its variables (to be denoted as the *potential*). The map f is an *exact symplectic twist* (see, for instance, [5]).

1.3 Lagrangian version

We can interpret the previous map as a discretization of some Hamiltonian equations. The Lagrangian point of view is given by the recurrence:

$$x_{k+1} - 2x_k + x_{k-1} = \Omega(x_k).$$

Hence, an orbit is determined by a sequence of angles $(x_k)_k \in \mathbf{R}^d$. Its *rotation vector* (or frequency vector) is defined as the following limit, if it exists:

$$\lim_{k\to\infty} \frac{x_k}{k}.$$

---

[*] Presented at the XIV Congreso de Ec. Diferenciales y Aplicaciones, Vic (Barcelona), September 1995.

1.4 Fixed points and periodic orbits

The set of fixed points of f, $Fix(f)$, is defined as:

$$Fix(f) = \{(x,y) \in \mathbf{T}^d \times \mathbf{R}^d / \ \Omega(x) = 0, y \in \mathbf{Z}^d\}.$$

Furthermore, if $(x,y) \in Per_n(f)$, that is, if it is a periodic point of period n, the rotation vector is $\frac{p}{n} \in \mathbf{Q}^d$ such that

$$F^n(x,y) = (x,y) + (p,0).$$

This is the equation to solve to look for periodic orbits of rotation vector $\frac{p}{n}$.

1.5 Standard-like maps and Poincaré maps

The maps we shall study are models of Poincaré maps of Hamiltonians defined on the $(d+1)$-cylinder (in angle-action coordinates: $\tilde{x} = (x_0, x)$ and $\tilde{y} = (y_0, y)$) with a double resonance:

$$H(x_0, x; y_0, y) = y_0 + \frac{1}{2}\|y\|_2^2 + \epsilon \sum_{k \in \mathbf{Z}^d} c_k(y) e^{2\pi <k,x> i} + \dots \ .$$

(The section through $x_0 = 0$ is equivalent to the time-unit map).

2 The standard map and the Froeschlé map

Two important examples of this type of maps are the *Chirikov standard map* [2] and the *Froeschlé map* [3].

2.1 The standard map

The standard map is defined on the 1-cylinder and is given by the potential

$$V_K(x) = -\frac{K}{(2\pi)^2}\cos(2\pi x)$$

and, hence, it reads as:

$$\left\{ \begin{array}{l} y' = y - \frac{K}{2\pi}\sin(2\pi x), \\ x' = x + y' \ (\mathrm{mod}\ 1). \end{array} \right.$$

2.2 The Froeschlé map

The Froeschlé map is defined on the 2-cylinder by using the potential

$$V_{K_1,K_2,\lambda}(x_1,x_2) = -\frac{1}{(2\pi)^2}(K_1\cos(2\pi x_1) + K_2\cos(2\pi x_2) + \lambda\cos(2\pi(x_1+x_2))).$$

Hence, it reads as:

$$\left\{ \begin{array}{l} y_1' = y_1 - \frac{K_1}{2\pi}\sin(2\pi x_1) - \frac{\lambda}{2\pi}\sin(2\pi(x_1+x_2)), \\ y_2' = y_2 - \frac{K_2}{2\pi}\sin(2\pi x_2) - \frac{\lambda}{2\pi}\sin(2\pi(x_1+x_2)), \\ x_1' = x_1 + y_1' \ (\mathrm{mod}\ 1), \\ x_2' = x_2 + y_2' \ (\mathrm{mod}\ 1). \end{array} \right.$$

2.3 Some particular cases in the Froeschlé map

We note that the Froeschlé map is the product of two standard maps plus some coupling. One has the following:

- If $\lambda = 0$, it is the product of two standard maps.
- If $K_1 = K_2 = 0$, it is the product of a rotation and a standard maps (of parameter 2λ).

Last claim is seen by using the change of variables:

$$\left\{ \begin{array}{ll} u_1 = x_1 - x_2, & v_1 = y_1 - y_2, \\ u_2 = x_1 + x_2, & v_2 = y_1 + y_2. \end{array} \right.$$

By this change, an orbit with rotation vector $\omega = (\omega_1, \omega_2)$ becomes another one with rotation vector $\bar{\omega} = (\omega_1 - \omega_2, \omega_1 + \omega_2)$.

We must point out that this is seen on $\mathbf{R}^2 \times \mathbf{R}^2$ and not on $\mathbf{T}^2 \times \mathbf{R}^2$, because such a change do not defines a diffeomorphism on the last manifold.

3 The KAM theory and the break down of invariant tori

Let us recall some results:

- If $\Omega = 0$, the map is

  $$\left\{ \begin{array}{l} x' = x + y \ (\mathrm{mod}\ 1), \\ y' = y, \end{array} \right. ,$$

  and each one of the tori $y = \omega$ is invariant. If ω is rational, then all the orbits in such a torus are periodic, while if it is irrational the orbits are dense. In both cases the rotation vector is defined (and it is equal to ω, of course).

- The *KAM Theory* (of Kolgomorov, Arnold and Moser) assures that, if the perturbation Ω of the previous system is sufficiently small, then most of the *invariant tori* subsist. The tori are labelled by their frequencies, the more badly approximable by rationals the rotation vector is, the more difficult is to broke the corresponding torus. This translates as some *diophantine condition* to be satisfied by the frequency vector.

- To obtain good estimates on the domain of existence of such tori, it is better to look at a concrete frequency vector. For the standard map (and similar maps), we can ask about the *critical value*, K_ω, needed in order that the curve corresponding to such frequency, ω, breaks (eventually, for the first time).

- Greene [4] proposed a method to answer the previous question, by looking to the *stability* of nearby periodic orbits. For instance, taking again the standard map one has:

  $$\begin{array}{lll} \omega = \frac{1}{2}(\sqrt{5} - 1) & \Rightarrow & K_\omega \approx 0.972, \\ \omega = (\sqrt{2} - 1) & \Rightarrow & K_\omega \approx 0.957, \\ \omega = (\sqrt{3} - 1) & \Rightarrow & K_\omega \approx 0.876. \end{array}$$

  A different approach, more based on the geometry of the *invariant manifolds* of nearby periodic points, was proposed by Olvera and Simó [6].

- While the break down of invariant curves is rather well understood (that is, the case of 2D maps), there are very few results concerning higher dimensions. Furthermore, the existing results refer to invariant tori which are *Lagrangian graphs*. (For instance, telling about the behaviour of periodic orbits close to an invariant torus of this kind [7]).

4 Approximation of invariant sets by periodic orbits

The approximation of invariant sets by periodic orbits can rely on the two next propositions. Before stating them we need to recall a few concepts (see, for instance, [1]):

- Given a metric space (X, d) one defines
$$\mathcal{H}(X) = \{K \subset X/\ K \neq \phi, K \text{ compact}\}.$$
- In the previous set one defines the *Hausdorff distance*, as
$$h(A, B) = \max(\rho(A, B), \rho(B, A)),$$
where
$$\rho(A, B) = \max_{a \in A} \min_{b \in B} d(a, b).$$

Let X and Y be two metric spaces and $f : X \rightarrow Y$ a continuous map. It induces a map $F : \mathcal{H}(X) \rightarrow \mathcal{H}(Y)$, defined by $F(K) = f(K)$ (we can thing of it as an extension of f). One obtains:

Theorem F is a continuous extension of f.

Let now $f : X \rightarrow X$ be a continuous map. We shall say that $K \subset X$ is (strictly) invariant by f if and only if $f(K) = K$. From the previous Theorem it follows the following

Corollary Let $(K_n)_n$ be a sequence of f-invariant nonempty compact sets, convergent to K (in the Hausdorff metric). Then:

K is f-invariant.

In particular, the limit of a sequence of periodic orbits, if it exists, is a compact invariant.

5 A numerical study of the break down of tori

We want to study the *break down* of an invariant torus with frequencies (ω_1, ω_2), which exists in the uncoupled case (we shall select the values of the K parameters less than the corresponding critical values). The process we shall use is as follows:

1. First one constructs a sequence of rational rotation vectors tending to the selected one. In this case one lacks the concept of continued fraction (whose convergents give the best approximations to an irrational number), but one can apply several 'reasonable' criteria.
2. For each of the constructed rational rotation vectors:
    - A periodic orbit for the product of standard maps is computed.
    - The orbit is continuated with respect to the coupling parameter, λ, as far as possible.

    In both cases we use the symmetries of the maps (they are reversible), to simplify the computations.
3. Then the angular components, (x_1, x_2), of the periodic orbits obtained, are drawn, and one can see the metamorphoses with respect to the parameter λ.
4. Finally, the drawings corresponding to the same value of the parameter λ (and different rational rotation vectors) are compared, to try to detect to which kind of object the sequence of periodic orbits seems to tend.

6 Reversible maps

Let X be a set and $T : X \to X$ a bijective transformation.
Let $I : X \to X$ an involutive map ($I^2 = id$).
We shall say that T is *I-reversible* (or that I is a *reversor* of T) if and only if $T^{-1} = ITI$.

For all $j \in \mathbf{Z}$, we define $I_j = T^j I$ and the j-th *symmetry axis* as

$$\Gamma_j = \{x \in X | I_j x = x\}.$$

Then we say that an orbit is *j-symmetric* if and only if it is invariant by I_j. The following holds:

- $x \in \Gamma_j,\ T^q x \in \Gamma_k,\ 2q + j - k \neq 0 \Rightarrow$
  x is $\mid 2q + j - k \mid$-periodic and $\theta(x)$ is symmetric with respect I_j and I_k.

In particular, if we look for n-periodic symmetric orbits, we can look for $x \in X$ such that:

- If $n = 2q$:
  $x \in \Gamma_0, T^q x \in \Gamma_0$ (symmetric with respect to I_0), or
  $x \in \Gamma_1, T^q x \in \Gamma_1$ (symmetric with respect to I_1).
- If $n = 2q + 1$:
  $x \in \Gamma_1, T^q x \in \Gamma_0$, or
  $x \in \Gamma_0, T^{q+1} x \in \Gamma_1$
  (in both cases symmetric with respect to I_0 and I_1).

7 Reversible standard-like maps and computation of symmetric periodic orbits

7.1 Reversible standard-like maps

In our case one has $f = I_1 I_0$, where:

$$I_0 = \left\{ \begin{array}{l} x' = -x \pmod 1 \\ y' = y + \Omega(x) \end{array} \right. ,\ I_1 = \left\{ \begin{array}{l} x' = -x + y \pmod 1 \\ y' = y \end{array} \right.$$

and in order that I_0 be an involution (I_1 already is) it is enough that Ω be an odd function.

Then, the (principal) symmetry axes of our reversible map are:

$$\Gamma_0 = \bigcup_{b \in \{0,1\}^d,\ \Omega(\frac{1}{2}b)=0} S_{0,b},\ \Gamma_1 = \bigcup_{b \in \{0,1\}^d} S_{1,b},$$

where $S_{a,b} = \{(\frac{1}{2}(ay + b), y)/\ y \in \mathbf{R}^d\} \subset \mathbf{T}^d \times \mathbf{R}^d$. To simplify we shall assume that all the symmetry 'sub-axes' exist:

$$\Omega(\frac{1}{2}b) = 0\ \forall b \in \{0, 1\}^d$$

(This is the case in the standard and Froeschlé maps).

7.2 Computation of symmetric periodic orbits

The search for symmetric periodic orbits of rotation vector $\frac{p}{n}$ is summarized by the following diagrama:

$$y \quad \rightarrow \quad (x = \tfrac{1}{2}(a_0 y + b_0), y) \quad \rightarrow (x_q, y_q) \quad \rightarrow \quad 2x_q - a_1 y_q - b_1,$$

where:

- $a_0 \in \{0,1\}, b_0 \in \{0,1\}^d$
- if n is even: $a_1 = a_0$
  if n is odd: $a_1 = 1 - a_0$
- $b_1 = b_0 + p$
- if n is even: $q = \frac{n}{2}$
  if n is odd and $a_0 = 0$: $q = \frac{n+1}{2}$
  if n is odd and $a_0 = 1$: $q = \frac{n-1}{2}$

Using this formulation the dimension of the problem is halved.

8 A parallel shooting technique to solve the equations

To solve an equation of the form

$$F^n(z) = z$$

is equivalent to solve the system:

$$\begin{cases} z_1 = F(z_0), \\ z_2 = F(z_1), \\ \vdots \\ z_0 = F(z_{n-1}). \end{cases}$$

This is the background of the methods developed, with the following variants:

- the symmetries of the problem have been used, and
- it is enough to consider the angular variables to determine the orbit.

Hence, it is possible to reduce the dimension of the problem to one fourth of the initial one. The advantages can be summarized in two items:

- in our case, the differential of F has spectral radius ≥ 1, and so, the differential of F^n can be extremely large if n is large, giving rise to accuracy problems;
- the continuation is more efficient.

9 A summary of results

The scheme given in section 5 has been implemented, taking as frequencies $\omega_1 = \sqrt{2}-1, \omega_2 = \sqrt{3}-1$ and different values of the parameters K_1, K_2. In particular, the following three cases have been considered:

1. In the first case small values of K_1 y K_2 are taken ($K_1 = K_2 = 10^{-5}$). It is known that for $K_1 = K_2 = 0$ the torus breaks for $\lambda \approx 0.31$, and, furthermore, is does so, obviously, in the form $\mathbf{T}^1 \times \mathcal{C}$, where $\mathcal{C}$ stands for a *Cantor set* in dimension 1. (We recall that in this case the map is a rotation times a standard map). For small values of K_1 and K_2 the break down must be of the same type, and this agrees with the experimental results displayed in figure 1.
2. In the second we have taken $K_1 = 0.94$ and $K_2 = 0.86$, close to the corresponding critical values, but less than them. For larger values the torus would break in the form $\mathcal{C} \times \mathcal{C}$. A similar thing must be expected. The experimental results displayed in figure 2 confirm this expectation.
3. Finally, the values $K_1 = 0.1$ and $K_2 = 0.2$ have been taken. When increasing λ a *resonance phenomenon* is observed (see figure 3), and the reason for that must be analyzed.

Notice that, in cases 1) and 3) (of type $\mathbf{T}^1 \times \mathcal{C}$) some strips of approximate slope -1 (obvius due to the change of variables introduced in **2** show up. In the case 2) (of type $\mathcal{C} \times \mathcal{C}$) they appear in a not so clear way.

Actually we are examining more cases using also larger periods. It is expected that the reasons for the different ways the tori break down are related to geometrical obstructions that can be seen as a generalization of the results given in the Olvera-Simó's paper. It seems that codimension 1 manifolds should play a key role.

Acknowledgements. This work has been partially supported by the CICYT grants ESP91–0403 / PB94–0215 and by the European Network grant ERBCHRXCT 940460.

References

[1] M. Barnsley. *Fractals everywhere.* Academic Press.

[2] B.V. Chirikov. *A universal instability of many-dimensional oscillator systems.* Phys. Rep. 52 (1979), p. 263.

[3] C. Froeschlé. *Numerical study of a four-dimensional mapping.* Astron. Astrophys. 16 (1972), p. 172.

[4] J.M. Greene. *A method for determining a stochastic transition.* J. Math. Phys. 20 (1979), p. 1183.

[5] J.D. Meiss. *Symplectic maps, variational principles, and transport.* Reviews of Modern Physics 64, no. 3 (1992), p. 795.

[6] A. Olvera and C. Simó. *An obstruction method for the destruction of invariant curves.* Physica D 26 (1987), p. 181.

[7] S. Tompaidis. *Approximation of invariant surfaces by periodic orbits in high-dimensional maps. Some rigorous results.* Presented at the NATO-ASI on Hamiltonian Systems with three or more degrees of freedom, S'Agaró (Catalunya, Spain), June 1995.

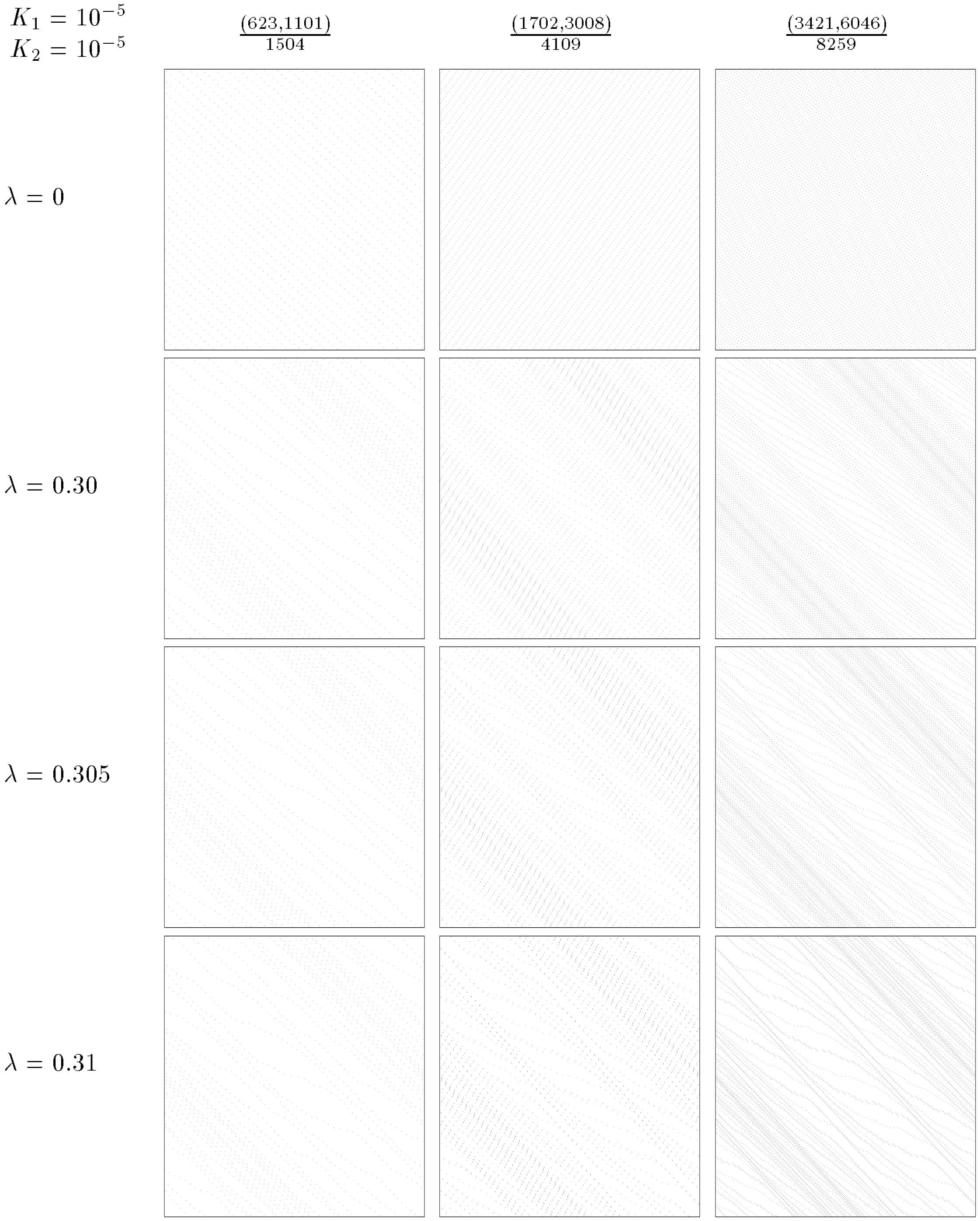
$K_1 = 10^{-5}$
$K_2 = 10^{-5}$
$\frac{(623,1101)}{1504}$
$\frac{(1702,3008)}{4109}$
$\frac{(3421,6046)}{8259}$
$\lambda = 0$
$\lambda = 0.30$
$\lambda = 0.305$
$\lambda = 0.31$

Figure 1

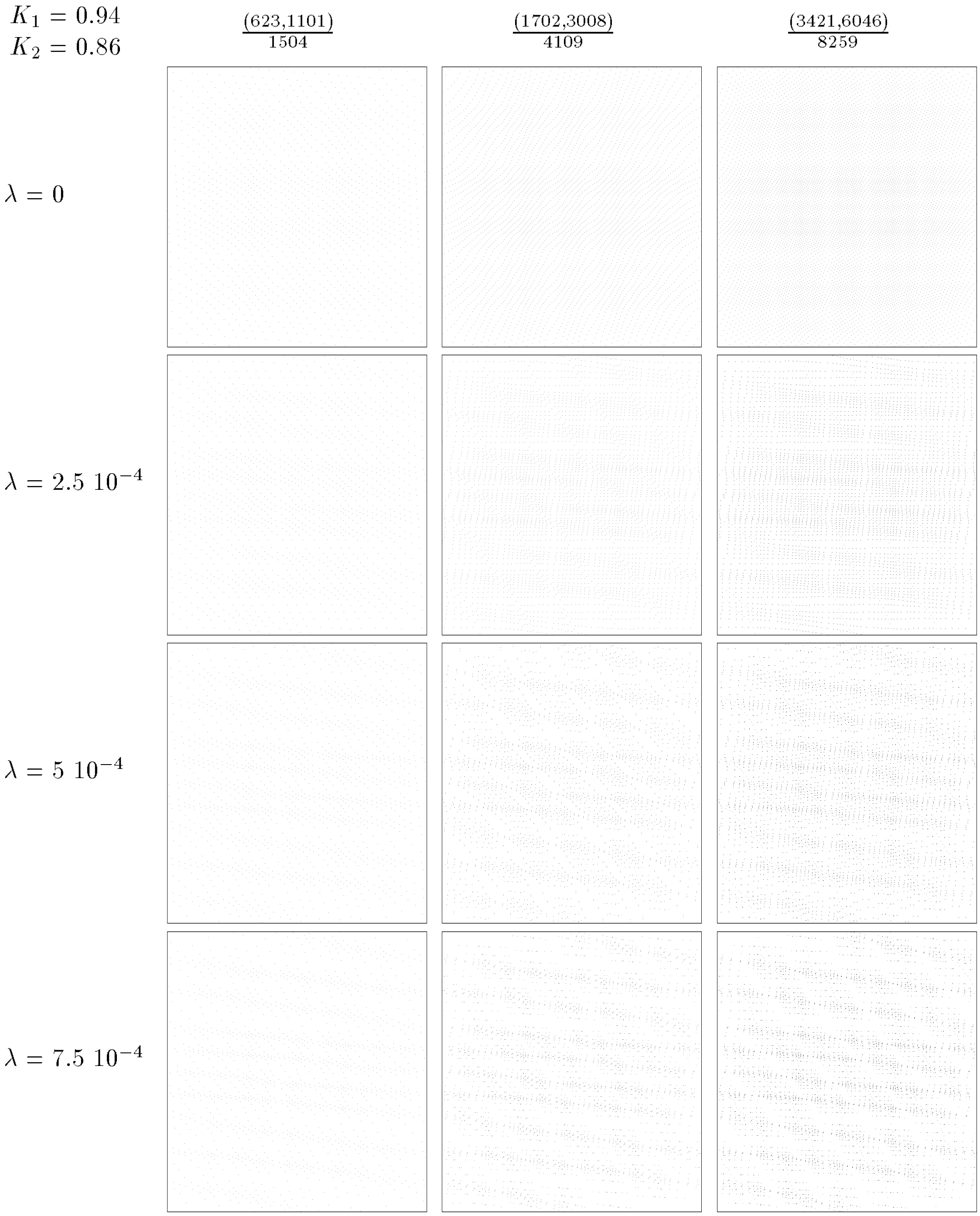
$K_1 = 0.94$
$K_2 = 0.86$
$\frac{(623,1101)}{1504}$
$\frac{(1702,3008)}{4109}$
$\frac{(3421,6046)}{8259}$
$\lambda = 0$
$\lambda = 2.5\ 10^{-4}$
$\lambda = 5\ 10^{-4}$
$\lambda = 7.5\ 10^{-4}$

Figure 2

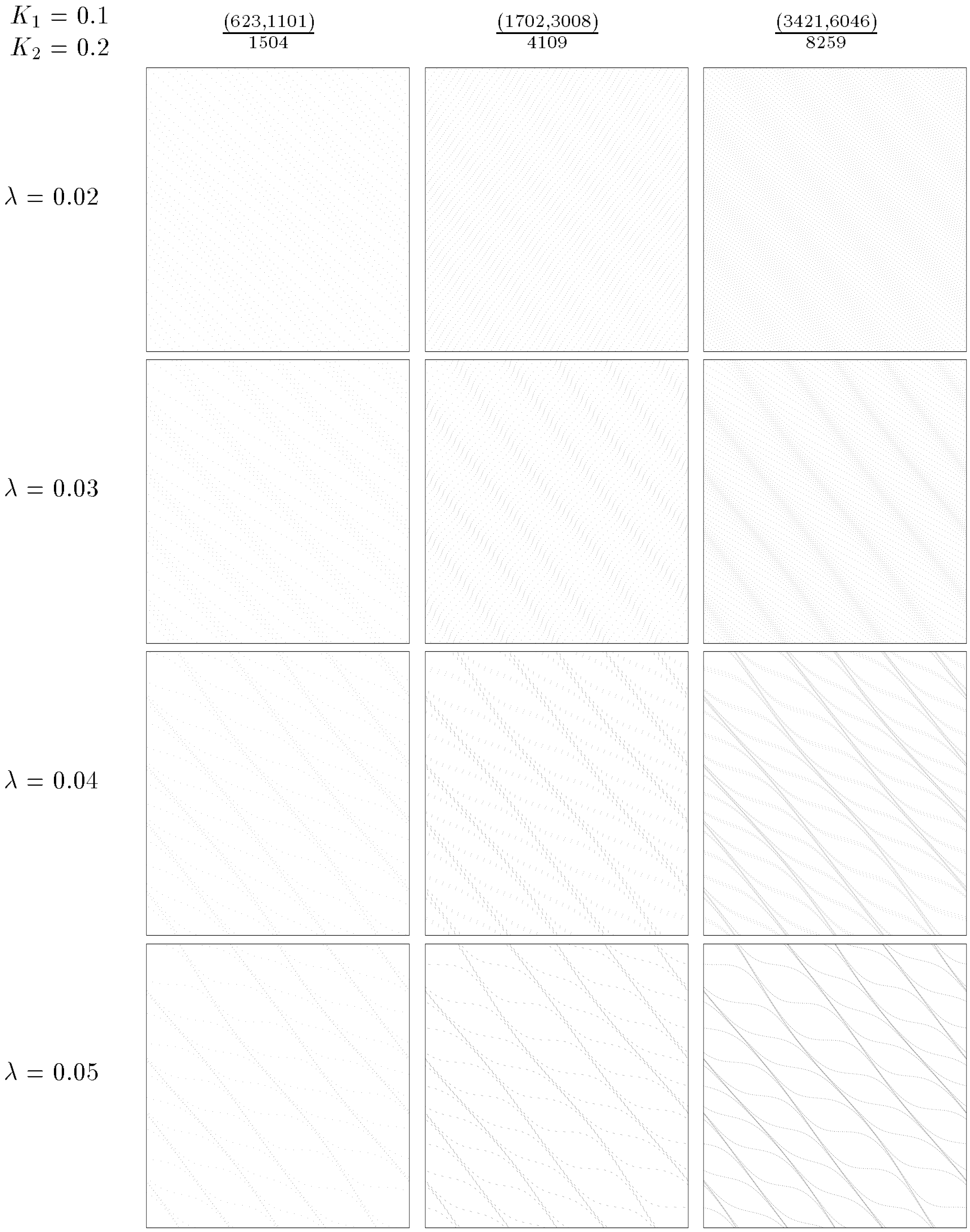
$K_1 = 0.1$
$K_2 = 0.2$
$\frac{(623,1101)}{1504}$
$\frac{(1702,3008)}{4109}$
$\frac{(3421,6046)}{8259}$
$\lambda = 0.02$
$\lambda = 0.03$
$\lambda = 0.04$
$\lambda = 0.05$

Figure 3